

# Timed Notch Inhibition Drives Photoreceptor Fate Specification in Human Retinal Organoids

Shereen H. Chew,<sup>1,2</sup> Cassandra Martinez,<sup>1,2</sup> Kathleen R. Chirco,<sup>1,3</sup> Sangeetha Kandoi,<sup>1,2</sup> and Deepak A. Lamba<sup>1,2</sup>

<sup>1</sup>Department of Ophthalmology, University of California San Francisco, California, United States

<sup>2</sup>Eli and Edythe Broad Center of Regeneration Medicine and Stem Cell Research, University of California San Francisco, California, United States

<sup>3</sup>Division of Neuroscience, Oregon National Primate Research Center, Oregon Health and Science University, Beaverton, Oregon, United States

Correspondence: Deepak A. Lamba, Department of Ophthalmology, University of California San Francisco, 35 Medical Center Way, San Francisco, CA 94143, USA; [deepak.lamba@ucsf.edu](mailto:deepak.lamba@ucsf.edu).

Received: May 23, 2022

Accepted: August 30, 2022

Published: September 21, 2022

Citation: Chew SH, Martinez C, Chirco KR, Kandoi S, Lamba DA. Timed notch inhibition drives photoreceptor fate specification in human retinal organoids. *Invest Ophthalmol Vis Sci.* 2022;63(10):12. <https://doi.org/10.1167/iovs.63.10.12>

**PURPOSE.** Transplanting photoreceptors from human pluripotent stem cell–derived retinal organoids have the potential to reverse vision loss in affected individuals. However, transplantable photoreceptors are only a subset of all cells in the organoids. Hence, the goal of our current study was to accelerate and synchronize photoreceptor differentiation in retinal organoids by inhibiting the Notch signaling pathway at different developmental time-points using a small molecule, PF-03084014 (PF).

**METHODS.** Human induced pluripotent stem cell– and human embryonic stem cell–derived retinal organoids were treated with 10  $\mu$ M PF for 3 days starting at day 45 (D45), D60, D90, and D120 of differentiation. Organoids were collected at post-treatment days 14, 28, and 42 and analyzed for progenitor and photoreceptor markers and Notch pathway inhibition by immunohistochemistry (IHC), quantitative PCR, and bulk RNA sequencing ( $n = 3–5$  organoids from three independent experiments).

**RESULTS.** Retinal organoids collected after treatment showed a decrease in progenitor markers (KI67, VSX2, PAX6, and LHX2) and an increase in differentiated pan-photoreceptor markers (OTX2, CRX, and RCVRN) at all organoid stages except D120. PF-treated organoids at D45 and D60 exhibited an increase in cone photoreceptor markers (RXRG and ARR3). PF treatment at D90 revealed an increase in cone and rod photoreceptors markers (ARR3, NRL, and NR2E3). Bulk RNA sequencing analysis mirrored the immunohistochemistry data and quantitative PCR confirmed Notch effector inhibition.

**CONCLUSIONS.** Timing the Notch pathway inhibition in human retinal organoids to align with progenitor competency stages can yield an enriched population of early cone or rod photoreceptors.

Keywords: notch inhibition, stem cells, organoids, photoreceptors, iPSCs

Most forms of retinal degeneration ultimately lead to the permanent loss of the light-sensing cells called photoreceptors. The human retina does not inherently regenerate and so the ensuing vision loss is permanent. Currently, there are no known effective therapeutics for the vast majority of these patients. However, as long as the inner retina stays intact, transplanting photoreceptors can provide an avenue to restore vision. Human pluripotent stem cells (hPSCs) have been used to generate retinal photoreceptors in a monolayer or organoid setting to study development and disease.<sup>1–4</sup> Alternatively, laboratory-generated photoreceptors could be used as a pool of photoreceptors for transplantation.<sup>5–8</sup> Over the course of development, retinal progenitor cells (RPCs) differentiate into their final cell fate in the neural retina, including cone and rod photoreceptors, retinal ganglion cells (RGCs), amacrine cells, horizontal cells, bipolar cells, and Müller glia.

One of the critical pathways maintaining RPC multipotency is the Notch pathway. It is a ligand-receptor pathway

that is used between multipotent cells to control neuronal potential and proliferation.<sup>9,10</sup> When the ligand (Delta-like or Jagged in mammals) from a neighboring cell interacts with the Notch receptor, it induces cleavage in Notch by ADAM-family metalloproteases (Fig. 1A).<sup>10</sup> The Notch intracellular domain is then cleaved by  $\gamma$ -secretase and activates the DNA-binding CSL protein, which complexes with Mastermind and other transcription factors, in the nucleus to express proliferation genes, such as *HES1* and *HES5* (Fig. 1A).<sup>10</sup> This process helps to maintain the RPC pool throughout retinal development. Notch signaling has been studied in many species to understand its importance in retinal differentiation and specification. Constitutive Notch pathway activation in the retina results in either a persistent progenitor state or differentiation into Müller glia.<sup>11</sup> Conversely, the inhibition of Notch signaling via small molecule  $\gamma$ -secretase inhibitors in mouse and chicken retina leads to synchronized differentiation of the tissue.<sup>12</sup> The Notch signaling pathway has also been implicated in retinal

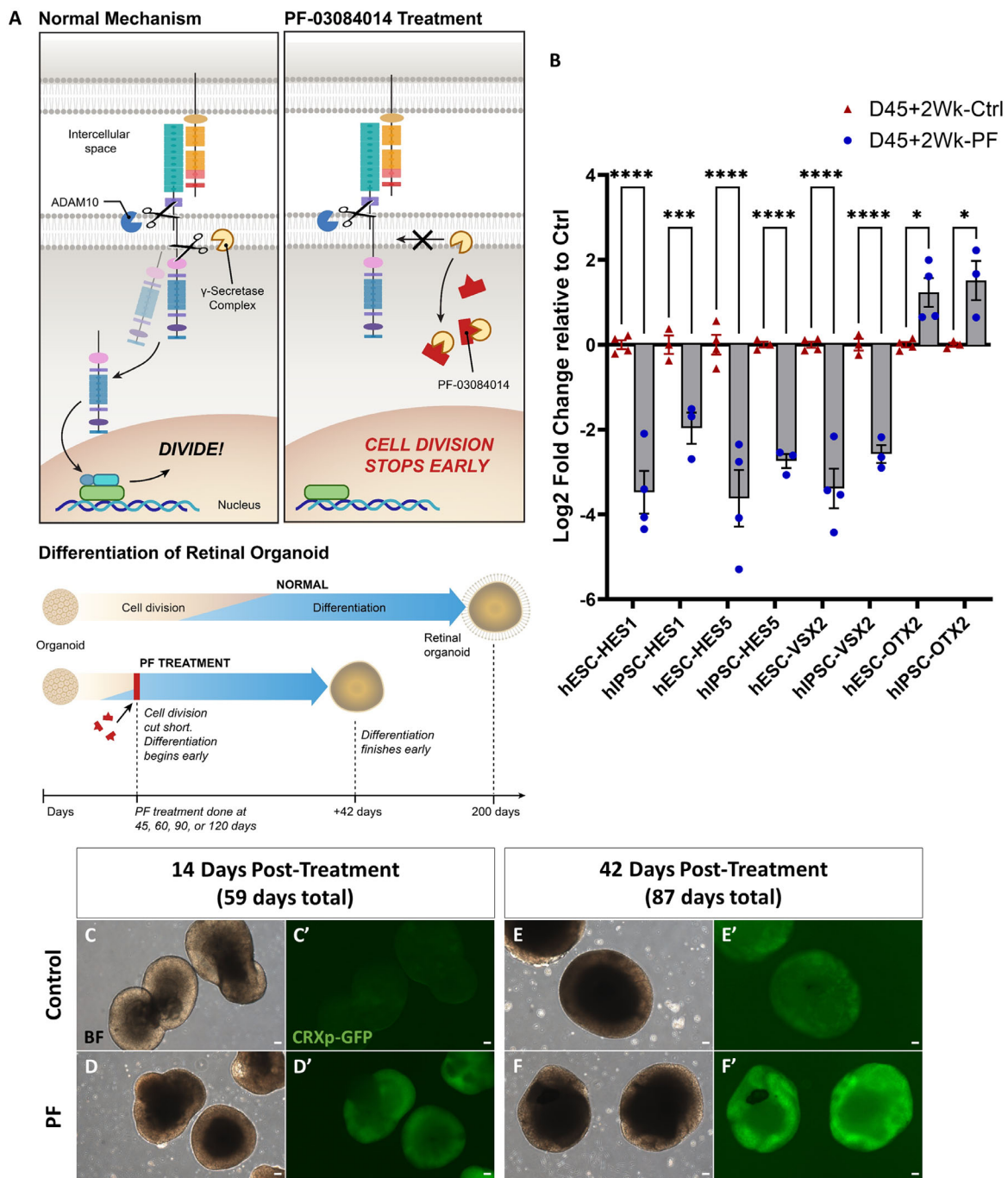


**FIGURE 1.** RPCs lose Notch activity after PF treatment and increase in photoreceptor fate. **(A)** Schematic of the Notch signaling pathway before and after treatment with PF. **(B)** Quantitative PCR data are shown for human embryonic stem cell (hESC) and human induced pluripotent stem cell lines after post-treatment day 14 as log<sub>2</sub> fold change compared with control organoids for *HES1*, *HES5*, *VSX2*, and *OTX2* ( $n = 5$  organoids per line, 3 biological replicates). **(C–F')** Bright-field and green fluorescent protein (GFP) expression observation in early retinal organoid generated from CRXp-GFP H9 hESCs. PF treatment started at D45. After 14 days, PF-treated (**D'**) organoids expressed more CRXp-GFP than their control counterparts (**C'**). This was also the case after 42 days (**E'**, **F'**). Scale bar, 50  $\mu\text{m}$ . \* $P < 0.05$ , \*\* $P < 0.01$ , \*\*\* $P < 0.005$ , \*\*\*\* $P < 0.001$ . All statistical analyses were performed using one-way ANOVA with a Dunnett test to correct for multiple comparisons in GraphPad Prism 9 software. See also Figure S1 for DAPT data. Ctrl, control.

regeneration: in *Xenopus* and chicken retina, Müller glia upregulate Notch signaling after damage and are critical to restore the progenitor potential.<sup>13,14</sup>

Dysregulated Notch signaling has been associated with a number of developmental and oncogenic disorders, including some forms of leukemia. As a result, drug-like molecules

have been developed for human therapies including  $\gamma$ -secretase inhibitors. PF-03084014 (PF) is a  $\gamma$ -secretase inhibitor used in conjunction with docetaxel in a phase I breast cancer therapy trial,<sup>15</sup> as well as desmoid tumors.<sup>16</sup> PF drove a decrease in endogenous Notch intracellular domain levels and a downregulation of Notch effector Hes1 in

T-cell acute lymphoblastic leukemia cell lines bearing Notch 1 translocation mutation as in patients. This process led to cell cycle arrest and eventually apoptosis.<sup>17</sup> Owing to its potent inhibition of the Notch pathway, we used PF to drive synchronized differentiation of RPCs in our retinal organoids.<sup>18</sup> Recently, a single cell ATAC-seq analysis of PF treatment of human fetal tissue showed a decrease in accessibility of regions bearing the RBPJ motif (Notch effector) and an increase in accessible regions with an OTX2 motif.<sup>19</sup> Because we know approximately when each of the retinal cell types are born from birth dating studies, we hypothesized that targeting the differentiation of specific cell types by using PF would generate an enriched pool of targeted cell types. These cells could then be used for transplantation or for studying molecular pathways that guide RPC differentiation. In this report, we describe our efforts of enriching photoreceptors from hPSC-derived retinal organoids using the Notch pathway inhibitor, PF. We show that early progenitors (before D60) are biased to generate cones, whereas late progenitors (beyond D90) are biased toward rods.

## EXPERIMENTAL PROCEDURES

### Cell Culture

The human embryonic stem cell line (CRXp-GFP H9) was kindly provided by Dr. Anand Swaroop. The iPSC line was kindly provided by Dr. Xianmin Zeng.<sup>20</sup> Cells were maintained on Matrigel (Corning 354234) coated plates in mTeSR1 medium (StemCell Technologies) or mTeSR Plus medium (StemCell Technologies) in a 5% CO<sub>2</sub>/5% O<sub>2</sub> incubator and passaged every 3 to 4 days using EDTA.

### Retinal Organoid Differentiation

Retinal organoids were differentiated via the embryoid body approach as described elsewhere.<sup>3</sup>

### Notch Inhibition

PF-03084014 (PF; Sigma Aldrich PZ0298-5MG) was prepared by dissolving it in DEPC water to a working concentration of 1 mM. Aliquots were stored at -80°C until use. On treatment day, organoids were treated with 10 μM PF dissolved in media. After 3 days, fresh non-PF media were given every 2 to 3 days until collection day. The reconstituted PF loses activity in approximately 3 months even at -80°C, so care was taken to use fresh compound. DAPT (Sigma Aldrich) was dissolved per manufacturer instructions and organoids treated with 50 μM for 2 days.

### Bulk RNA Sequencing Data Analysis

Control and PF-treated organoids were collected at 28 days after treatment for mRNA extraction for RNA-seq analysis (see Supplementary Methods). Library preparation and Illumina-based transcriptome sequencing was carried out at Novogene. After quality control (error rates of <0.03%), alignments were parsed using STAR (v2.5) program<sup>79</sup> and mapped to the *Homo sapiens* genome assembly GRCh37 (hg19). Heatmaps of key genes was graph using BEAVR web package (v1.0.10)<sup>80</sup> in Docker. Differential expressions were determined through DESeq2 R package (v1.14.1).<sup>81</sup> Genes with an adjusted *P* value of less than 0.05 found

by DESeq2 were assigned as differentially expressed. Data were graphed in R using the Enhanced Volcano plots package.<sup>82</sup> Gene ontology enrichment analysis of differentially expressed genes was carried out by ClusterProfiler R package (v2.4.3),<sup>83</sup> in which gene length bias was corrected.

## RESULTS

### Small Molecule $\gamma$ -Secretase Inhibitor Blocks Notch Pathway Activity in Three-dimensional Retinal Organoids and Drives Differentiation

Using previously published three-dimensional retinal organoid differentiation protocols,<sup>3,4</sup> we generated organoids from a human induced pluripotent stem cell line<sup>20</sup> and a modified human embryonic stem cell line (CRXp-GFP H9<sup>21</sup>). Both lines consistently made retinal organoids, signified by a bright outer ring of retinal tissue. D45 organoids were then treated with 10 μM of the  $\gamma$ -secretase inhibitor, PF-03084014 hydrobromide, for 3 days and analyzed at post-treatment day 14 (D59) for downstream effectors of Notch (*HES1* and *HES5*) and early retina genes (*VSX2* and *OTX2*) using quantitative PCR. Both *HES1* and *HES5* have been shown to be downstream of Notch and are important regulators in neuronal differentiation.<sup>22</sup> *VSX2* is expressed in developing RPCs, but is downregulated as cells differentiate, except in bipolars and Müller glia.<sup>23,24</sup> *OTX2* is expressed in photoreceptors, bipolars, and RPE.<sup>25,26</sup> We observed a consistent decrease in downstream Notch pathway targets (*HES1* and *HES5*) (Fig. 1B) in organoids from both cell lines after PF treatment. This finding was associated with a decrease in RPC genes (*VSX2*). Concomitantly, we observed an increase in the photoreceptor gene (*OTX2*) (Fig. 1B). Interestingly, DAPT, another Notch  $\gamma$ -secretase inhibitor, which has been used to inhibit Notch in chickens and mice retina,<sup>12,13</sup> did not drive significant differentiation (Supplementary Fig. S1). These data indicate that the clinically relevant Notch pathway inhibitor PF drives differentiation of human RPCs.

CRX is an essential transcription factor that regulates many downstream photoreceptor genes.<sup>25-27</sup> The CRXp-GFP H9 reporter line, generated to report activity of *CRX* promoter in differentiating photoreceptors, has been shown to express GFP around D37 in retinal organoids.<sup>21</sup> This reporter line allowed us to estimate the timing of photoreceptor differentiation *in vitro* (Figs. 1C-F). At 14 (Fig. 1D) and 42 days (Fig. 1F) post-D45 treatment, we observed significantly higher GFP expression compared with control cultures (Figs. 1C'-E') along with loss of typical bright organoid appearance on brightfield (Figs. 1D, F). Thus, PF treatment drove CRX expression, suggesting that the organoids were pushed toward a photoreceptor fate.

### PF-Treated Retinal Organoids Lose Progenitor Properties in Early Time Points

Because PF treatment had a profound effect on driving differentiation in D45 retinal organoids, we next tested the effects on RPCs at different developmental stages (D45, 60, 90, and 120) and analyzed them using immunohistochemistry (IHC) after 14 and 42 days (Fig. 2A). Overall, we observed an almost complete loss in KI67, a pan cell cycle



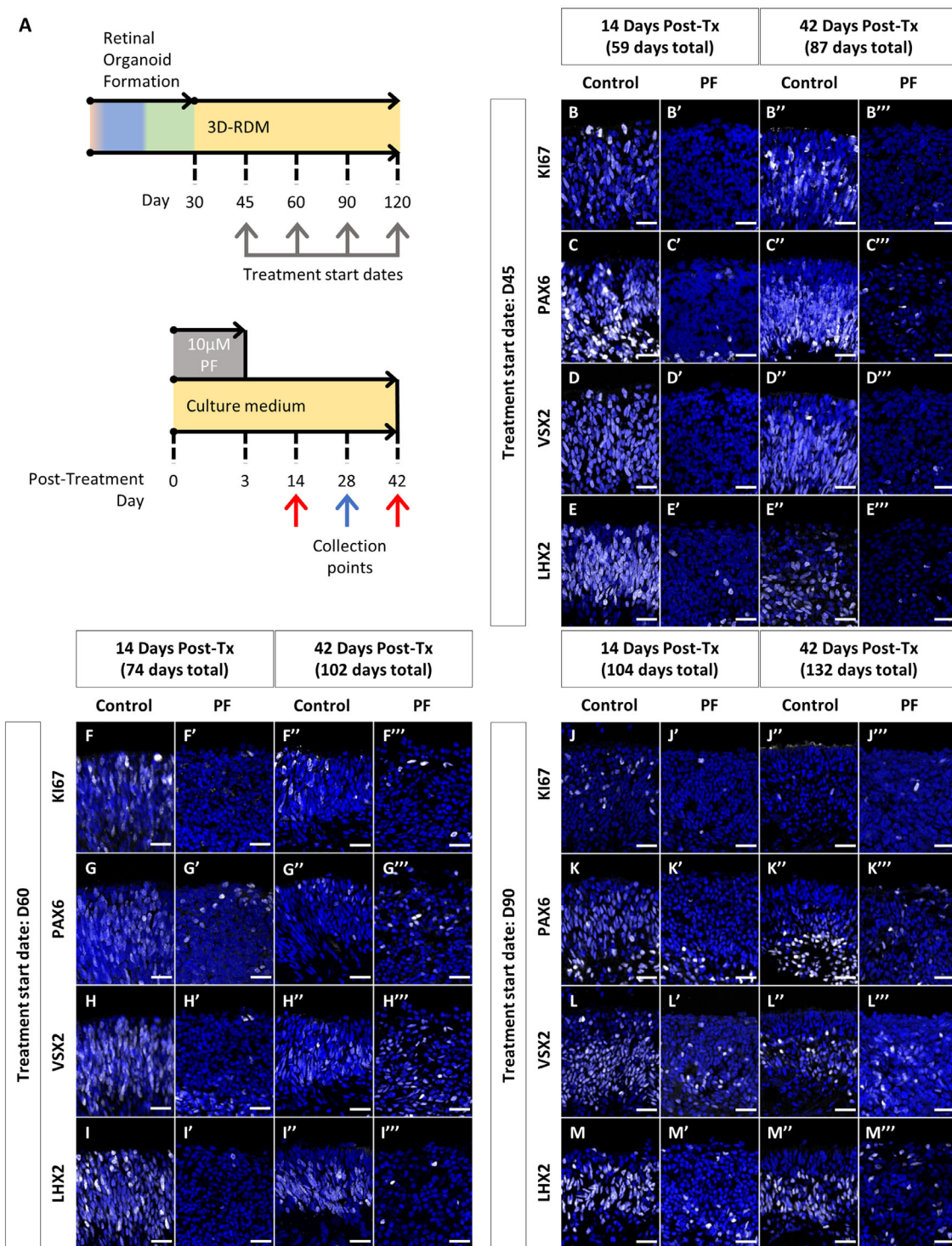


**FIGURE 2.** Notch inhibition turns off progenitor markers in retinal organoids. (A) Schematic of the treatment timeline. Once RPCs are generated on day 30, separate PF treatment occurred on D45, 60, 90, and 120. Collections for IHC happened after 14 and 42 days (red arrows) and for bulk RNA-seq after 28 days (blue arrow). (B–M) Immunofluorescence staining using antibodies against KI67 (B, F, J), PAX6 (C, G, K), VSX2 (D, H, L), LHX2 (E, I, M) are shown in white for treatment groups D45 (B–E), D60 (F–I), and D90 (J–M). Nuclei are counterstained with DAPI in blue. Scale bar, 25 µm. See also Figure S2 for quantitative data and Figure S3 for the D120 treatment group.

marker expressed in the nuclei of proliferating cells,<sup>28</sup> at 14 days for the D45, D60, and D90 treatment groups (Figs. 2B, F, J, Supplementary Fig. S2). Interestingly, there were few KI67<sup>+</sup> cells (3.3% ± 1.5%) in the D60 42 days post-PF group than the D60 14 days post-PF organoids (0.4% ± 0.4%). This

finding could be due to some PF treatment-resistant cells that continued to proliferate afterward. Finally, D90 organoids at 42 days control conditions have few KI67<sup>+</sup> cells (4.7% ± 1.63%) that are lost upon PF treatment (0.9% ± 0.45%). The D120 group do not have any KI67<sup>+</sup> cells after 14 and 42 days

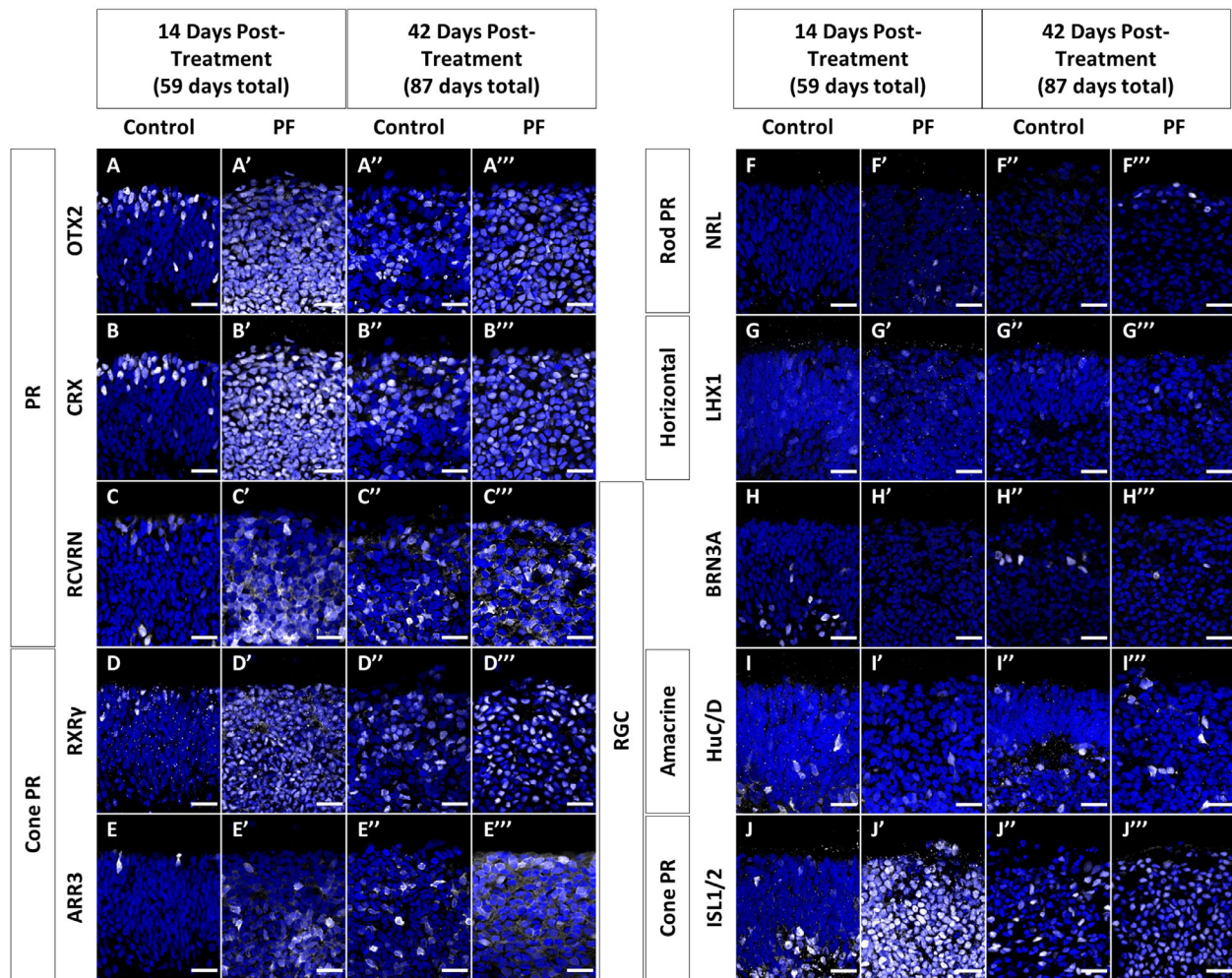


**FIGURE 3.** Notch inhibition at D45 causes mass generation of immature cone photoreceptors in retinal organoids after 14 and 42 days. Immunofluorescence staining using antibodies against OTX2 (A), CRX (B), RCVRN (C), RXR $\gamma$  (D), ARR3 (E), NRL (F), LHX1 (G), BRN3A (H), HuC/D (I), and ISL1/2 (J) are shown in white. Markers are split into pan photoreceptors (A–C), cones (D, E, J), rods (F), horizontals (G), RGCs (H–J), and amacrine (I). Nuclei are counterstained with DAPI in blue. Scale bar, 25  $\mu$ m. See also Figure S2 for quantitative data and Figures S4–5 for additional staining data.

(Supplementary Fig. S3A), suggesting that the organoids are fully differentiated by D134.

We further confirmed our KI67 data with other specific RPC markers such as PAX6, VSX2, and LHX2. We observed a consistent loss of expression of these proteins in the neuroblastic layers in the D45, D60, D90, and D120 groups after treatment (Figs. 2C–E, 2G–I, 2K–M, Supplementary Figs. S2, 3B–D). Although PAX6 was expressed in the organoids, there were clear groups of PAX6<sup>high</sup> and PAX6<sup>low</sup> cells. These PAX6<sup>high</sup> cells likely correspond with amacrine, as well as RGCs, although they tend to die off in later stages of organoid development.<sup>29–31</sup> VSX2<sup>low</sup> cells were abundantly present in controls, but decrease to a few rare VSX2<sup>low</sup> after PF treatment (Figs. 2C, G, K, Supplementary Figs. S2, S3B); the post-treatment cells are most likely bipolars, indicated by VSX2<sup>high</sup> expression (Figs. 2D'–D''', H'–H''', L'–L''', Supplementary Figs. S3C'–C''').<sup>24</sup> The same was true for remaining LHX2<sup>+</sup> Müller glia at this stage (Figs. 2E, I, M, Supplementary Fig. S3D).<sup>32</sup> The D120 organoids contained predominantly LHX2<sup>high</sup> cells (Supplementary Fig. S3D), indicating the absence of any significant RPCs at this time-point.

### Notch Knockdown Increases Cone Photoreceptor Population in Early-Stage Retinal Progenitors

Because PF treatment results in synchronized differentiation of human RPCs in the retinal organoids, we next sought to test the competency of RPCs to generate various retinal neurons. Birth-dating studies have closely correlated genesis of different retinal neurons to progenitor staging.<sup>33–39</sup> Based on these, cones are poised to be generated in D45 to D60 retinal organoids. To investigate cone photoreceptor development, we immunostained for OTX2, CRX, RCVRN, RXR $\gamma$ , and ARR3. Recoverin (RCVRN) is a Ca<sup>2+</sup>-binding protein that helps to regulate the phosphorylation of the visual opsins in photoreceptors.<sup>40,41</sup> RXR $\gamma$  is present in developing cones and is downregulated to form S-cone photoreceptors.<sup>21,42</sup> ARR3 aids in quenching the phosphorylated state of S- and M/L-opsins in cone photoreceptors.<sup>43</sup> The D45 post 14-day control group had a few cells that are positive for OTX2, CRX, RCVRN, RXR $\gamma$ , and ARR3 (Figs. 3A–E, Supplementary Fig. S2A), which increased over the next 4 weeks. Upon PF treatment, at the 14-day time-point, we observed that the majority of cells expressed OTX2, CRX, and RXR $\gamma$ ,



along with significant increases in RCVRN (Figs. 3A–D', Supplementary Fig. S2A). At the 42-day time-point, again we observed similar changes in the above proteins (Figs. 3A–D, Supplementary Fig. S2A). Additionally, ARR3, which was higher at the 14-day time-point after treatment compared with controls, was further upregulated at 42 days after PF treatment (Figs. 3E–E'''), suggesting further maturation of the cone photoreceptors. Interestingly, although we see a massive increase in photoreceptor differentiation, the typical multilayered retinal alignment is lost.

Although it is not anticipated, we wanted to assess whether D45 RPCs were competent to generate any rod photoreceptors. NRL is necessary and sufficient to form rod photoreceptors.<sup>44</sup> We observed no NRL<sup>+</sup> cells in either D45 14 and 42 days control groups (Figs. 3F, F''). Surprisingly, after PF treatment, a few rare NRL<sup>+</sup> rod photoreceptors were observed in the D45 14- and 42-day post-treatment groups (Figs. 3F', F''', Supplementary Fig. S2A), suggesting that even D45 retinal organoids have minor competence to generate rod photoreceptors.

Birth-dating studies suggest that early retinal progenitors have the potential to generate RGCs, amacrine, and horizontal cells.<sup>34–37,45</sup> We next tested the ability to generate these cells in D45 organoids after PF treatment. LHX1 is expressed by developing horizontals,<sup>46</sup> and we observed few scattered LHX1<sup>+</sup> horizontals in control organoids (Figs. 3G, G''), with no significant change upon PF treatment at both the 14- and 42-day time-points (Figs. 3G', G'''). BRN3, a POU4F transcription factor family present in RGCs in the retina, determines the diversity of RGCs.<sup>47</sup> Most of the BRN3A<sup>+</sup> (POU4F1) cells are present in the lower one-half or below of the neuroblastic layer in the 14- and 42-day controls (Figs. 3H, H''). Interestingly, after PF treatment, we detected very few, if any, BRN3A<sup>+</sup> cells in the organoids (Figs. 3H', H''', Supplementary Fig. S2A). This finding suggests that either the RGCs are struggling to survive in a mature organoid model lacking stem or glial cell support or that PF is directly toxic to RGCs in the organoids. HuC/D is expressed by mature RGCs and amacrine and in developing horizontals (in rats).<sup>48</sup> We found a large population of HuC/D<sup>+</sup> cells in the 14-day control conditions (Fig. 3I), but the number of cells diminished modestly after treatment (Fig. 3I'). The 42-day control and treated groups show similar expression of HuC/D<sup>+</sup> cells (Figs. 3I''–I'''). Given the observed pattern of BRN3A<sup>+</sup> cells (Fig. 3H), it is likely that most of the HuC/D<sup>+</sup> cells are amacrine in treated organoids and do not change with PF treatment. Finally, ISL1 is expressed in RGCs, amacrine, and bipolars whereas ISL2 is in cones.<sup>49,50</sup> Staining for ISL1/2, we observed a dramatic increase in ISL1/2<sup>+</sup> cells in the 14-day treated group compared with the corresponding control (Figs. 3J–J'), with an expression pattern similar to OTX2 and CRX staining (Figs. 3A, B), suggesting that most of these might be early cone photoreceptors. At the 42-day time-point, there was not much change between the control and treated groups (Figs. 3J''–J'''). This finding could be due to only a transient expression in ISL2 in newly differentiated cones.<sup>51</sup> To test whether the cellular competency changed significantly in D60 organoids, we next treated these with PF for 3 days and analyzed them 14 and 42 days later. Here again, we observed that PF resulted in a cone-rich organoid (Figs. 4A–E, Supplementary Fig. S2B), without any significant changes in the other cell types (Figs. 4F–H, Supplementary Fig. S2B).

One of the most intriguing findings was a lack of maturity in the cone photoreceptors in the PF-treated differentiated

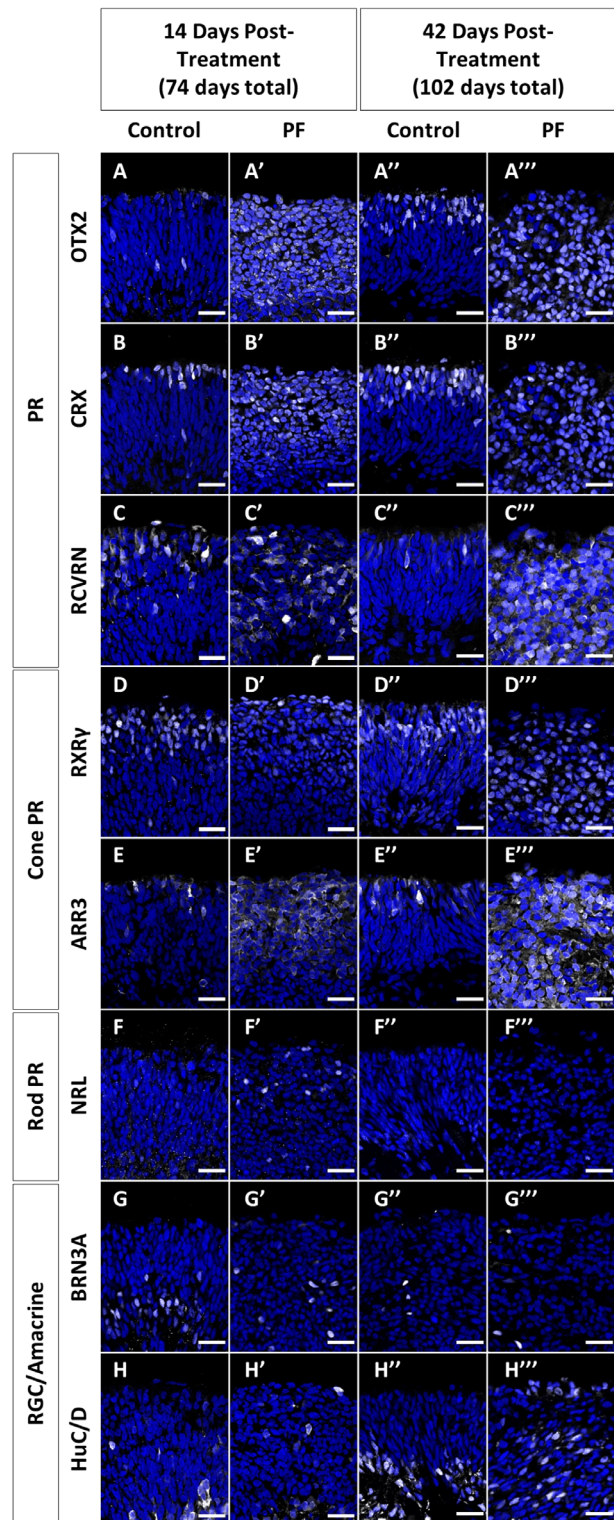


**FIGURE 4.** Notch inhibition at D60 causes mass generation of immature cone photoreceptors in retinal organoids after 14 and 42 days. Immunofluorescence staining using antibodies against OTX2 (A), CRX (B), RCVRN (C), RXR $\gamma$  (D), ARR3 (E), NRL (F), BRN3A (G), and HuC/D (H) are shown in white. Markers are split into pan photoreceptors (A–C), cones (D, E), rods (F), and RGC/amacrine (G–I). Nuclei are counterstained with DAPI in blue. Scale bar, 25  $\mu$ m. See also Figure S2 for quantitative data and Figures S4–5 for additional staining data.

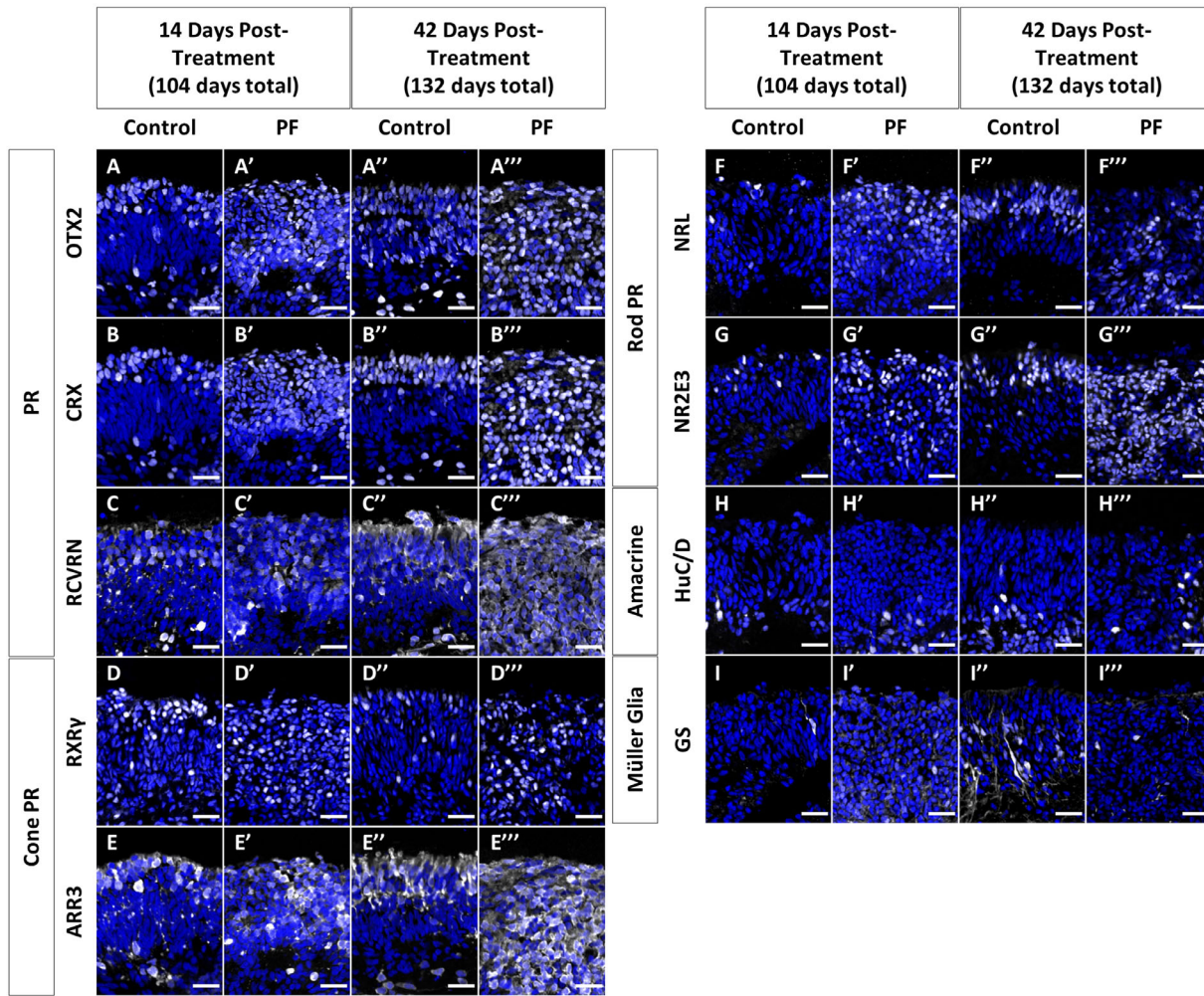


**FIGURE 5.** Notch inhibition at D90 causes mass generation of immature rod photoreceptors in retinal organoids after 14 and 42 days. Immunofluorescence staining using antibodies against OTX2 (A), CRX (B), RCVRN (C), RXR $\gamma$  (D), ARR3 (E), NRL (F), NR2E3 (G), HuC/D (H), and glutamine synthase (I) are shown in white. Markers are split into pan photoreceptors (A–C), cones (D, E), rods (F, G), amacrine (H), and Müller glia (I). Nuclei are counterstained with DAPI in blue. Scale bar, 25  $\mu$ m. See also Figure S2 for quantitative data and Figures S4–5 for additional staining data.

organoids. S- and M/L-opsins are required for cone photoreceptors to be able to process photons into a chemical signal. There was a lack of S- and M/L-opsins expression in both the D45 and D60 14- and 42-day post-treatment groups (Supplementary Figs. S4A, B, D, E). Even upon further culture for 70 and 140 days after treatment on D45, organoids failed to express either of the opsins (Supplementary Figs. S5A, B). Furthermore, these PF-treated organoids do not express rod markers despite long-term culture, owing to the absence of competence at this stage (Supplementary Figs. S5C–E). These data suggest that, although PF can drive cone-rich organoids, accelerating the *in vitro* culture system lacks the cues required to complete the maturation of photoreceptors.

### Notch Knockdown in Late Retinal Progenitors Increases the Rod Photoreceptor Population

Late retinal progenitors are biased to generate rod photoreceptors over cones.<sup>34–37,45,52</sup> To examine our ability to stimulate rod photoreceptor generation, we cultured retinal

organoids for 90 days before a 3-day PF treatment. At 14 and 42 days after treatment, general photoreceptor protein makers (OTX2, CRX, and RCVRN) increased in both PF-treated groups compared with control (Figs. 5A–C''', Supplementary Fig. S2C). Cone photoreceptor expression also increased as shown by RXR $\gamma$  and ARR3 immunolabeling (Figs. 5D–E''', Supplementary Fig. S2C). Next, we looked for the generation of rod photoreceptors using rod-specific markers, namely, NRL<sup>44,53</sup> and NR2E3.<sup>52,54</sup> We found a significant increase in both rod markers at 14 days after PF treatment and even more so after 42 days (Figs. 5F–G''', Supplementary Fig. S2C). Based on these data, D90 organoids are both rod and cone photoreceptor competent. HuC/D<sup>+</sup> amacrine remained toward the bottom of the neuroblastic layer and did not increase after PF treatment (Figs. 5H–H''').

Müller glia are the last retinal cell type formed from RPCs and Notch signaling is an important driver for Müller glia formation.<sup>55–57</sup> Müller glia are identified by glutamine synthase (GS) expression.<sup>58</sup> In D90 control organoids, Müller glia start to form but are sparse (Fig. 5I). Interestingly, we observed a reduction in number of GS<sup>+</sup> Müller glia espe-



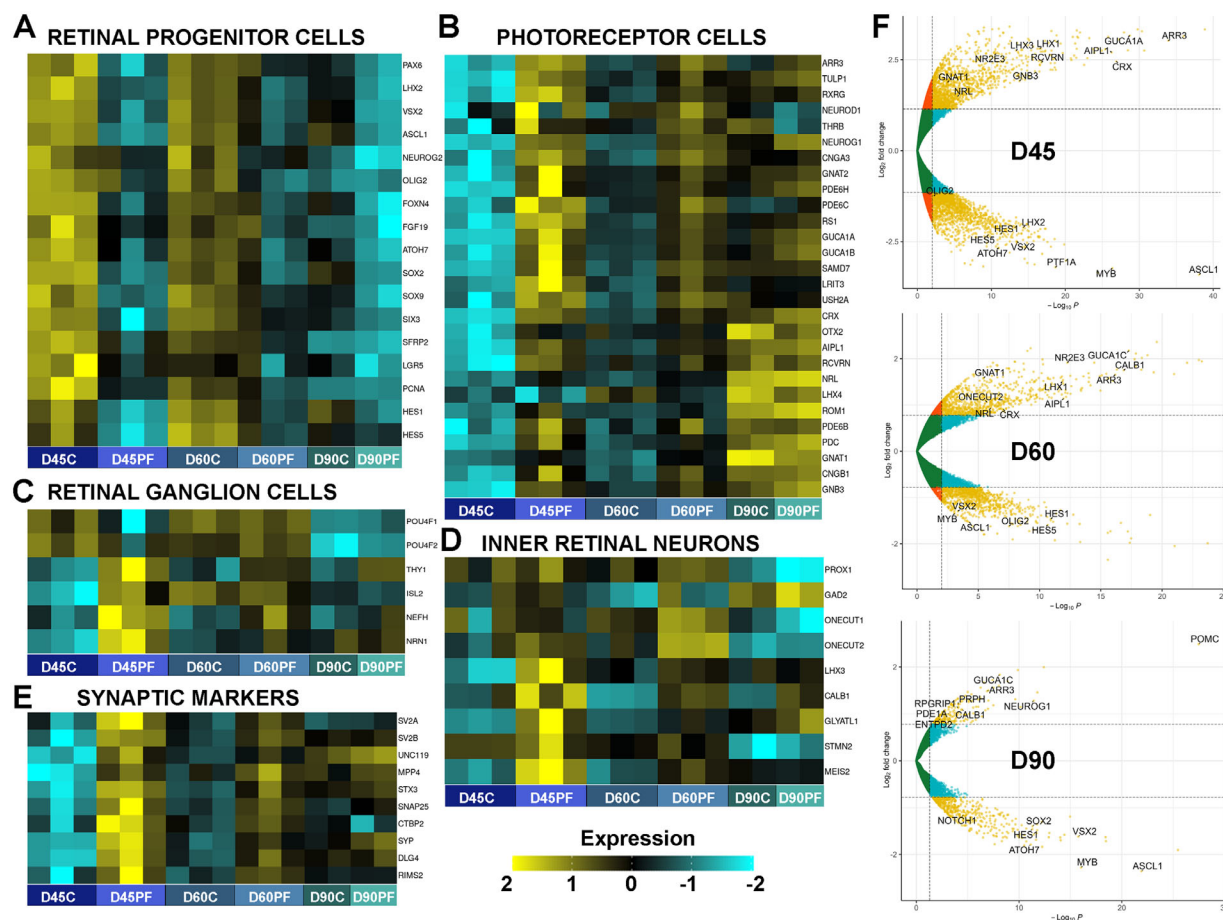


**FIGURE 6.** RNA sequencing analysis of PF treated retinal organoids confirm RPC loss and photoreceptor differentiation phenotypes. Organoids were treated for 3 days at D45, D60, and D90 of differentiation and analyzed 28 days later. **(A)** At all three stages there is a consistent downregulation of RPC genes and Notch pathway effectors with a stronger effect at early time-points when the organoids are RPC enriched. **(B)** Photoreceptor genes are highly upregulated especially at D45 and D60 treatment time-points. Smaller increases in rod-specific genes were observed in the D90 treatment group. **(C)** RGC specification genes (*POU4F* family) were downregulated while maturation markers upregulated with PF. **(D)** Smaller increases in inner retina specification genes were observed while maturation markers were highly upregulated. **(E)** PF treatment led to the consistent upregulation of various synaptic maturation genes expressed in the inner and outer retina. **(F)** Volcano plot showing the significant differentially expressed genes at all three treatment time-points. See also Figure S6 for additional RNA-seq analysis.

cially at the 42-day post-treatment time point (Figs. 5I'–I'''). This PF-mediated decrease in Müller glia is most likely due to the lack of Notch signaling needed for their specification.

In the D120 treatment group, where we did not observe any change in progenitor expression after PF (Supplementary Figs. S3A–D'''), there were no significant changes in expression for photoreceptor markers (*OTX2*, *CRX*, *RCVRN*, and *ARR3*; Supplementary Figs. S3E–H'''). A small number of M/L-opsin<sup>+</sup> cells were observed in the 42-day control and treated organoids (Supplementary Figs. S3I'–I'''), but this finding is most likely due to the age of the organoids and not a result of the treatment. The number of NRL<sup>+</sup> rod photoreceptor cells were unchanged at 14 days after PF with a small increase at 42 days (Supplementary Figs. S3J'–J''').

### RNA Sequencing Analysis of PF-treated Organoids

We next sought to analyze the effects of Notch inhibition using bulk RNA-seq analysis. We cultured retinal organoids for either 45, 60, or 90 days before 3 days of PF treatment as described elsewhere in this article. At 28 days after treat-

ment, RNA was collected and processed for RNA-seq analysis. This time-point was chosen as a midpoint between the two time-points included in the IHC analysis. Upon analysis of Notch pathway effector (*HES1* and *HES5*) expression, we observed a significant downregulation at all three stages of differentiation, with the maximal downregulation in the D45 treatment group (Fig. 6A). This is likely because the organoids at this stage have the most RPCs with active intercellular Notch activity compared with the other treatment time-points. Similarly, we confirmed the downregulation of various genes typically expressed in RPCs, including *PAX6*, *LHX2*, *VSX2*, *ASCL1*, and *SOX2* (Fig. 6A). In alignment with our IHC data, cone photoreceptor differentiation was biased in early-stage organoids (D45 and D60) as evidenced by increases in *ARR3*, *RXRG*, *TULP1*, *GNAT2*, *CNGA3*, and *PDE6C*, among other cone genes (Fig. 6B).

In contrast, D90 PF-treated organoids were rod photoreceptor biased, with smaller differences in marker expression levels compared with untreated organoids at this age (D118); RPCs have mostly differentiated at this time-point, and control cultures have generated rods as well (Fig. 6B).



We observed relatively small changes in rod maturation genes (*ROM1*, *NRL*, and *GNB3*).

Similar to our IHC data (Fig. 3), we observed a downregulation of RGC markers, *POU4F1* (BRN3A) and *POU4F2* (BRN3B), in the D45 and D90 treatment groups; however, we did see an increase in maturation genes typically associated with RGCs (*THY1*, *NEFH*, and *NRN1*) at all three time-points (Fig. 6C). These increases in RGC markers could be due to an increase in expression in surviving RGCs or cross-expression in other inner retinal neurons. Next, we focused on other inner retinal markers such as *PROX1*, which mark progenitors destined to interneuron fates (e.g., amacrine and horizontals).<sup>59</sup> *PROX1* was increased in D60 PF-treated organoids, suggesting an increase in the pool of amacrine and horizontals at this time-point (Fig. 6D). This finding was further confirmed by the elevated expression of both *ONECUT2* and *ONECUT1*, which both regulate early born cell fates and are critical for horizontal cell genesis,<sup>60,61</sup> and *GAD2*, *GLYTLL1A*, *MEIS2*, and *STMN2*, which are linked to amacrine and horizontal cell fates<sup>62–65</sup> (Fig. 6D). One of our surprising findings was the early upregulation of *LHX3* post-PF treatment at D45 and, to a lesser extent, D60 (Fig. 6D). *LHX3* in rodent species has been linked to bipolar differentiation<sup>66–68</sup>; however, we hypothesize that *LHX3* may be a transiently expressed marker of early retinal cell fates, such as cone photoreceptors. Finally, we analyzed cellular maturation through using synaptic markers.<sup>69</sup> We observed significant upregulation of a number of photoreceptors and pan-retina associated synaptic genes (e.g., *SV2*, *SNAP25*, *SYP*, and *RIMS2*), especially in D45 and D60 treatment groups, with smaller changes in D90 treated organoids (Fig. 6E).

To confirm whether these changes were significant, we carried out differential expression analysis using DESeq2 analysis in R. Differential expression analysis confirmed our IHC data (Fig. 6F). At all three time points (D45, D60, and D90), we observed a significant decrease in Notch targets and RPC genes. D45-treated cells had the largest and most significant increase in photoreceptor associated genes. D90 had fewer significantly different genes and mostly enriched in photoreceptor maturation genes. A gene ontology analysis of the RNA-seq data showed that the most significant effect of PF treatment on retinal organoids was a downregulation of cell cycle, mitosis, and DNA replication, which in turn resulted in a significant increase in gene networks associated with visual perception and synaptic organization and activity (Supplementary Fig. S6).

## DISCUSSION

In this study, we describe a methodology to exploit human retinal progenitor competency states in retinal organoids to drive enriched photoreceptor populations. We show that the Notch pathway is active in RPCs within hPSC-derived retinal organoids, and that this pathway can be effectively inhibited using the Notch inhibitor, PF-03084014. Using this approach, we generated highly enriched cultures of photoreceptors with significantly decreased numbers of proliferating retinal stem cells. The broader goal of this work is to generate a more uniform source of photoreceptors that can be used for cell replacement therapies to aid in visual recovery.

The most unanticipated and interesting finding in our studies was the photoreceptor bias in our synchronized differentiated retinal organoids. When treated early (D45

or D60), we observed a significant increase in the cone population, shown via both IHC and bulk RNA-seq. The same phenomenon occurred with the rod photoreceptors when organoids were treated at D90, although to a smaller extent. Although we expected a noticeable increase in other inner retinal neurons after PF treatment, our data showed no significant differences to inner retinal neuron markers in PF-treated organoids, even at the D60 treatment time-point group. These results do, however, align well with previous studies showing that *Notch1* plays a role in the inhibition of cone and rod fate.<sup>11,70,71</sup> Conditional genetic knockdown of Notch in early RPCs in mice has been shown to result in cone overproduction at the expense of other retinal neurons, whereas a later-onset knockdown results in rod overproduction. Recent studies using well-defined cis-regulatory elements for various progenitor states, including *VSX2* for multipotent RPCs and *THRB* for cone-restricted RPCs, to analyze the effects of Notch signaling inhibition suggest that Notch regulates the formation of restricted RPC states from multipotent RPCs.<sup>72</sup> This potential mechanism could be driving specific fate decisions in human retina development. Additionally, Notch activity has been shown to be critical for the final Müller glia fate specification.<sup>55–57</sup> Persistent Notch activity promotes the expression of downstream Müller glial genes and stabilizes Müller glia fate.<sup>73</sup> Consistent with these studies, PF-treated retinal organoids show a paucity of Müller glia.

Another interesting aspect of our studies was a lack of complete maturation of the differentiated cone and rod photoreceptors. Although these cells expressed early cone and rod differentiation markers, including *RCVRN* and *ARR3*, the more mature markers, such as the opsins, were lacking in these prematurely differentiated cells despite long-term culture for 70 and 140 days after treatment. Similar observations have been made in Zebrafish Notch knockdown studies.<sup>57</sup> Together, these data suggest that other native retina cell types may be critical for driving the full maturation of photoreceptors, either directly or through secreted factors that may be missing in our PF-treated organoids. Recently, a number of factors have been shown to induce photoreceptor maturation and opsin expression in retinal organoids, including 9-cis retinaldehyde, docosahexaenoic acid, fibroblast growth factor-1, and thyroid hormone.<sup>74–76</sup> It remains to be seen whether the addition of these factors could potentially drive maturation in PF-treated organoids. Along with a lack of maturation, there was an obvious loss of lamination and impaired organization in the PF-treated organoids. We hypothesize that this is due to the absence of critical cues from RPCs and/or Müller glia, which likely provide spatial information to newly differentiated neurons. This factor also likely contributes to the lack of photoreceptor maturation, including the development of inner and outer segments. That being said, one advantage of generating an enriched pool of immature photoreceptors is that these cells will likely achieve better integration after transplantation, compared with more mature photoreceptors.<sup>77,78</sup>

In summary, the results reported herein show that Notch signaling is necessary for RPC maintenance in hPSC-derived retinal organoids. Notch pathway inhibition using a small molecule validated in human studies, PF-03084014, can drive photoreceptor specific synchronized differentiation in retinal organoids to generate enriched cultures of immature cone and rod photoreceptors, which could then be useful for cell replacement approaches to treat severe photoreceptor degenerative disorders in affected patients.

## Data Availability

RNA-seq raw data is available on NCBI GEO (GSE212640).

## Acknowledgments

The authors thank the members of the Lamba laboratory for helpful discussions and suggestions. The authors also thank Suling Wang for her assistance in creating Figure 1A.

Supported by the National Eye Institute (U24 EY029891 and R01 EY032197 to DAL; P30 [EY002162] Vision Core grant to UCSF Department of Ophthalmology), and the Research to Prevent Blindness (unrestricted grant to UCSF Department of Ophthalmology).

Disclosure: **S.H. Chew**, None; **C. Martinez**, None; **K.R. Chirco**, None; **S. Kandoi**, None; **D.A. Lamba**, None

## References

- Lamba DA, MO Karl, Ware CB, Reh TA. Efficient generation of retinal progenitor cells from human embryonic stem cells. *Proc Natl Acad Sci USA*. 2006;103(34):12769–12774, doi:10.1073/pnas.0601990103.
- Zhu J, Reynolds J, Garcia T, et al. Generation of transplantable retinal photoreceptors from a current good manufacturing practice-manufactured human induced pluripotent stem cell line: transplantable photoreceptors from cGMP iPSCs. *STEM CELLS Transl Med*. 2018;7(2):210–219, doi:10.1002/sctm.17-0205.
- Chirco KR, Chew S, Moore AT, Duncan JL, Lamba DA. Allele-specific gene editing to rescue dominant CRX-associated LCA7 phenotypes in a retinal organoid model. *Stem Cell Rep*. 2021;16(11):2690–2702, doi:10.1016/j.stemcr.2021.09.007.
- Ohlemacher SK, Sridhar A, Xiao Y, et al. Stepwise differentiation of retinal ganglion cells from human pluripotent stem cells enables analysis of glaucomatous neurodegeneration: hPSC-derived RGCs and glaucoma. *STEM CELLS*. 2016;34(6):1553–1562, doi:10.1002/stem.2356.
- Zhu J, Cifuentes H, Reynolds J, Lamba DA. Immunosuppression via loss of IL2 $\gamma$  enhances long-term functional integration of hESC-derived photoreceptors in the mouse retina. *Cell Stem Cell*. 2017;20(3):374–384.e5, doi:10.1016/j.stem.2016.11.019.
- Gagliardi G, Ben M, Barek K, Chaffiol A, et al. Characterization and transplantation of CD73-positive photoreceptors isolated from human iPSC-derived retinal organoids. *Stem Cell Rep*. 2018;11(3):665–680, doi:10.1016/j.stemcr.2018.07.005.
- Lin B, McLelland B, Xue Y, et al. hESC-derived retina organoids produced by a scalable cGMP compatible process improve visual function after transplantation to immunodeficient RD rats. *Invest Ophthalmol Vis Sci*. 2020;61(7):2505.
- Shirai H, Mandai M, Matsushita K, et al. Transplantation of human embryonic stem cell-derived retinal tissue in two primate models of retinal degeneration. *Proc Natl Acad Sci USA*. 2016;113(1):E81–E90, doi:10.1073/pnas.1512590113.
- Arai MA, Akamine R, Tsuchiya A, et al. The Notch inhibitor cowanin accelerates nicastrin degradation. *Sci Rep*. 2018;8(1):5376, doi:10.1038/s41598-018-23698-4.
- Bray SJ. Notch signalling: a simple pathway becomes complex. *Nat Rev Mol Cell Biol*. 2006;7(9):678–689, doi:10.1038/nrm2009.
- Jadhav AP, Cho SH, Cepko CL. Notch activity permits retinal cells to progress through multiple progenitor states and acquire a stem cell property. *Proc Natl Acad Sci USA*. 2006;103(50):18998–19003, doi:10.1073/pnas.0608155103.
- Nelson BR, Hartman BH, Georgi SA, Lan MS, Reh TA. Transient inactivation of Notch signaling synchronizes differentiation of neural progenitor cells. *Dev Biol*. 2007;304(2):479–498, doi:10.1016/j.ydbio.2007.01.001.
- Hayes S, Nelson BR, Buckingham B, Reh TA. Notch signaling regulates regeneration in the avian retina. *Dev Biol*. 2007;312(1):300–311, doi:10.1016/j.ydbio.2007.09.046.
- Raymond PA, Barthel LK, Bernardos RL, Perkowski JJ. Molecular characterization of retinal stem cells and their niches in adult zebrafish. *BMC Dev Biol*. 2006;6:36, doi:10.1186/1471-213X-6-36.
- Curigliano G, Aftimos PG, Dees EC, et al. Phase I dose-finding study of the gamma secretase inhibitor PF-03084014 (PF-4014) in combination with docetaxel in patients (pts) with advanced triple-negative breast cancer (TNBC). *J Clin Oncol*. 2015;33(15 Suppl):1068–1068, doi:10.1200/jco.2015.33.15\_suppl.1068.
- Kummar S, O'Sullivan Coyne G, Do KT, et al. Clinical activity of the  $\gamma$ -secretase inhibitor PF-03084014 in adults with desmoid tumors (aggressive fibromatosis). *J Clin Oncol*. 2017;35(14):1561–1569, doi:10.1200/JCO.2016.71.1994.
- Wei P, Walls M, Qiu M, et al. Evaluation of selective gamma-secretase inhibitor PF-03084014 for its antitumor efficacy and gastrointestinal safety to guide optimal clinical trial design. *Mol Cancer Ther*. 2010;9(6):1618–1628, doi:10.1158/1535-7163.MCT-10-0034.
- Kaufman ML, Park KU, Goodson NB, et al. Transcriptional profiling of murine retinas undergoing semi-synchronous cone photoreceptor differentiation. *Dev Biol*. 2019;453(2):155–167, doi:10.1016/j.ydbio.2019.05.016.
- Finkbeiner C, Ortuño-Lizarán I, Sridhar A, Hooper M, Petter S, Reh TA. Single-cell ATAC-seq of fetal human retina and stem-cell-derived retinal organoids shows changing chromatin landscapes during cell fate acquisition. *Cell Rep*. 2022;38(4):110294, doi:10.1016/j.celrep.2021.110294.
- Pei Y, Sierra G, Sivapatham R, Swistowski A, Rao MS, Zeng X. A platform for rapid generation of single and multiplexed reporters in human iPSC lines. *Sci Rep*. 2015;5(1):9205, doi:10.1038/srep09205.
- Kaewkhaw R, Kaya KD, Brooks M, et al. Transcriptome dynamics of developing photoreceptors in three-dimensional retina cultures recapitulates temporal sequence of human cone and rod differentiation revealing cell surface markers and gene networks: transcriptome of developing human photoreceptors. *Stem Cells*. 2015;33(12):3504–3518, doi:10.1002/stem.2122.
- Ohtsuka T, Ishibashi M, Gradwohl G, Nakanishi S, Guillemot F, Kageyama R. Hes1 and Hes5 as notch effectors in mammalian neuronal differentiation. *EMBO J*. 1999;18(8):2196–2207, doi:10.1093/emboj/18.8.2196.
- Livne-Bar I, Pacal M, Cheung MC, et al. Chx10 is required to block photoreceptor differentiation but is dispensable for progenitor proliferation in the postnatal retina. *Proc Natl Acad Sci USA*. 2006;103(13):4988–4993, doi:10.1073/pnas.0600083103.
- Vitorino M, Jusuf PR, Maurus D, Kimura Y, ichi Higashijima S, Harris WA. Vsx2 in the zebrafish retina: restricted lineages through derepression. *Neural Dev*. 2009;4(1):14, doi:10.1186/1749-8104-4-14.
- Glubrecht DD, Kim JH, Russell L, Bamforth JS, Godbout R. Differential CRX and OTX2 expression in human retina and retinoblastoma. *J Neurochem*. 2009;111(1):250–263, doi:10.1111/j.1471-4159.2009.06322.x.
- Yamamoto H, Kon T, Omori Y, Furukawa T. Functional and evolutionary diversification of Otx2 and Crx in vertebrate retinal photoreceptor and bipolar cell development.



- Cell Rep.* 2020;30(3):658–671.e5, doi:10.1016/j.celrep.2019.12.072.
27. Ruzycski PA, Zhang X, Chen S. CRX directs photoreceptor differentiation by accelerating chromatin remodeling at specific target sites. *Epigenetics Chromatin.* 2018;11(1):42, doi:10.1186/s13072-018-0212-2.
  28. Pacal M, Bremner R. Mapping differentiation kinetics in the mouse retina reveals an extensive period of cell cycle protein expression in post-mitotic newborn neurons. *Dev Dyn.* 2012;241(10):1525–1544, doi:10.1002/dvdy.23840.
  29. Marquardt T, Ashery-Padan R, Andrejewski N, Scardigli R, Guillemot F, Gruss P. Pax6 Is required for the multipotent state of retinal progenitor cells. *Cell.* 2001;105(1):43–55, doi:10.1016/S0092-8674(01)00295-1.
  30. Nishina S, Kohsaka S, Yamaguchi Y, et al. PAX6 expression in the developing human eye. *Br J Ophthalmol.* 1999;83(6):723–727.
  31. Shaham O, Menuchin Y, Farhy C, Ashery-Padan R. Pax6: a multi-level regulator of ocular development. *Prog Retin Eye Res.* 2012;31(5):351–376, doi:10.1016/j.preteyeres.2012.04.002.
  32. de Melo J, Zibetti C, Clark BS, et al. Lhx2 Is an essential factor for retinal gliogenesis and Notch signaling. *J Neurosci.* 2016;36(8):2391–2405, doi:10.1523/JNEUROSCI.3145-15.2016.
  33. Sridhar A, Hoshino A, Finkbeiner CR, et al. Single-cell transcriptomic comparison of human fetal retina, hPSC-derived retinal organoids, and long-term retinal cultures. *Cell Rep.* 2020;30(5):1644–1659.e4, doi:10.1016/j.celrep.2020.01.007.
  34. Bassett EA, Wallace VA. Cell fate determination in the vertebrate retina. *Trends Neurosci.* 2012;35(9):565–573, doi:10.1016/j.tins.2012.05.004.
  35. Brzezinski JA, Reh TA. Photoreceptor cell fate specification in vertebrates. *Development.* 2015;142(19):3263–3273, doi:10.1242/dev.127043.
  36. Cepko C. Intrinsically different retinal progenitor cells produce specific types of progeny. *Nat Rev Neurosci.* 2014;15(9):615–627, doi:10.1038/nrn3767.
  37. Xiang M. Intrinsic control of mammalian retinogenesis. *Cell Mol Life Sci.* 2013;70(14):2519–2532, doi:10.1007/s00018-012-1183-2.
  38. Hoshino A, Ratnapriya R, Brooks MJ, et al. Molecular anatomy of the developing human retina. *Dev Cell.* 2017;43(6):763–779.e4, doi:10.1016/j.devcel.2017.10.029.
  39. Boije H, MacDonald RB, Harris WA. Reconciling competence and transcriptional hierarchies with stochasticity in retinal lineages. *Curr Opin Neurobiol.* 2014;27:68–74, doi:10.1016/j.conb.2014.02.014.
  40. Bazhin AV, Schadendorf D, Philippov PP, Eichmüller SB. Recoverin as a cancer-retina antigen. *Cancer Immunol Immunother.* 2007;56(1):110–116, doi:10.1007/s00262-006-0132-z.
  41. Makino CL, Dodd RL, Chen J, et al. Recoverin regulates light-dependent phosphodiesterase activity in retinal rods. *J Gen Physiol.* 2004;123(6):729–741, doi:10.1085/jgp.200308994.
  42. Roberts MR, Hendrickson A, McGuire CR, Reh TA. Retinoid X receptor (gamma) is necessary to establish the S-opsin gradient in cone photoreceptors of the developing mouse retina. *Invest Ophthalmol Vis Sci.* 2005;46(8):2897–2904, doi:10.1167/iovs.05-0093.
  43. Sakuma H, Murakami A, Fujimaki T, Inana G. Isolation and characterization of the human X-arrestin gene. *Gene.* 1998;224(1):87–95, doi:10.1016/S0378-1119(98)00510-1.
  44. Mears AJ, Kondo M, Swain PK, et al. Nrl is required for rod photoreceptor development. *Nat Genet.* 2001;29(4):447–452, doi:10.1038/ng774.
  45. Boije H, Shirazi Fard S, Edqvist PH, Hallböök F. Horizontal cells, the odd ones out in the retina, give insights into development and disease. *Front Neuroanat.* 2016;10:77. Accessed January 19, 2022. <https://www.frontiersin.org/article/10.3389/fnana.2016.00077>.
  46. Liu W, Wang JH, Xiang M. Specific expression of the LIM/Homeodomain protein Lim-1 in horizontal cells during retinogenesis. *Dev Dyn.* 2000;217(3):320–325, doi:10.1002/(SICI)1097-0177(200003)217:3<320::AID-DVDY10>3.0.CO;2-F.
  47. Badea TC, Cahill H, Ecker J, Hattar S, Nathans J. Distinct roles of transcription factors Brn3a and Brn3b in controlling the development, morphology, and function of retinal ganglion cells. *Neuron.* 2009;61(6):852–864, doi:10.1016/j.neuron.2009.01.020.
  48. Ekström P, Johansson K. Differentiation of ganglion cells and amacrine cells in the rat retina: correlation with expression of HuC/D and GAP-43 proteins. *Dev Brain Res.* 2003;145(1):1–8, doi:10.1016/S0165-3806(03)00170-6.
  49. Elshatory Y, Everhart D, Deng M, Xie X, Barlow RB, Gan L. Islet-1 controls the differentiation of retinal bipolar and cholinergic amacrine cells. *J Neurosci.* 2007;27(46):12707–12720, doi:10.1523/JNEUROSCI.3951-07.2007.
  50. Martín-Partido G, Francisco-Morcillo J. The role of Islet-1 in cell specification, differentiation, and maintenance of phenotypes in the vertebrate neural retina. *Neural Regen Res.* 2015;10(12):1951–1952, doi:10.4103/1673-5374.165301.
  51. Fischer AJ, Foster S, Scott MA, Sherwood P. The transient expression of LIM-domain transcription factors is coincident with the delayed maturation of photoreceptors in the chicken retina. *J Comp Neurol.* 2008;506(4):584–603, doi:10.1002/cne.21578.
  52. O'Brien KMB, Cheng H, Jiang Y, Schulte D, Swaroop A, Hendrickson AE. Expression of photoreceptor-specific nuclear receptor NR2E3 in rod photoreceptors of fetal human retina. *Invest Ophthalmol Vis Sci.* 2004;45(8):2807–2812, doi:10.1167/iovs.03-1317.
  53. Akimoto M, Cheng H, Zhu D, et al. Targeting of GFP to newborn rods by Nrl promoter and temporal expression profiling of flow-sorted photoreceptors. *Proc Natl Acad Sci USA.* 2006;103(10):3890–3895, doi:10.1073/pnas.0508214103.
  54. Peng GH, Ahmad O, Ahmad F, Liu J, Chen S. The photoreceptor-specific nuclear receptor Nr2e3 interacts with Crx and exerts opposing effects on the transcription of rod versus cone genes. *Hum Mol Genet.* 2005;14(6):747–764, doi:10.1093/hmg/ddi070.
  55. Furukawa T, Mukherjee S, Bao ZZ, Morrow EM, Cepko CL. rax, Hes1, and notch1 promote the formation of Müller glia by postnatal retinal progenitor cells. *Neuron.* 2000;26(2):383–394, doi:10.1016/S0896-6273(00)81171-x.
  56. Hojo M, Ohtsuka T, Hashimoto N, Gradwohl G, Guillemot F, Kageyama R. Glial cell fate specification modulated by the bHLH gene Hes5 in mouse retina. *Development.* 2000;127(12):2515–2522, doi:10.1242/dev.127.12.2515.
  57. Bernardos RL, Lentz SI, Wolfe MS, Raymond PA. Notch-Delta signaling is required for spatial patterning and Müller glia differentiation in the zebrafish retina. *Dev Biol.* 2005;278(2):381–395, doi:10.1016/j.ydbio.2004.11.018.
  58. Linsler P, Moscona AA. Induction of glutamine synthetase in embryonic neural retina: localization in Müller fibers and dependence on cell interactions. *Proc Natl Acad Sci USA.* 1979;76(12):6476–6480, doi:10.1073/pnas.76.12.6476.
  59. Dyer MA, Livesey FJ, Cepko CL, Oliver G. Prox1 function controls progenitor cell proliferation and horizontal cell genesis in the mammalian retina. *Nat Genet.* 2003;34(1):53–58, doi:10.1038/ng1144.
  60. Klimova L, Antosova B, Kuzelova A, Strnad H, Kozmik Z. Onecut1 and Onecut2 transcription factors operate down-

- stream of Pax6 to regulate horizontal cell development. *Dev Biol.* 2015;402(1):48–60, doi:10.1016/j.ydbio.2015.02.023.
61. Sapkota D, Chintala H, Wu F, Fliesler SJ, Hu Z, Mu X. Onecut1 and Onecut2 redundantly regulate early retinal cell fates during development. *Proc Natl Acad Sci USA.* 2014;111(39):E4086–4095, doi:10.1073/pnas.1405354111.
  62. Bumsted-O'Brien KM, Hendrickson A, Haverkamp S, Ashery-Padan R, Schulte D. Expression of the homeodomain transcription factor Meis2 in the embryonic and postnatal retina. *J Comp Neurol.* 2007;505(1):58–72, doi:10.1002/cne.21458.
  63. Crooks J, Kolb H. Localization of GABA, glycine, glutamate and tyrosine hydroxylase in the human retina. *J Comp Neurol.* 1992;315(3):287–302, doi:10.1002/cne.903150305.
  64. Lu Y, Shiao F, Yi W, et al. Single-cell analysis of human retina identifies evolutionarily conserved and species-specific mechanisms controlling development. *Dev Cell.* 2020;53(4):473–491.e9, doi:10.1016/j.devcel.2020.04.009.
  65. Nakazawa T, Nakano I, Furuyama T, Morii H, Tamai M, Mori N. The SCG10-related gene family in the developing rat retina: persistent expression of SCLIP and stathmin in mature ganglion cell layer. *Brain Res.* 2000;861(2):399–407, doi:10.1016/s0006-8993(00)02056-4.
  66. Kim Y, Lim S, Ha T, et al. The LIM protein complex establishes a retinal circuitry of visual adaptation by regulating Pax6  $\alpha$ -enhancer activity. *eLife.* 2017;6:e21303, doi:10.7554/eLife.21303.
  67. Buenaventura DF, Corseri A, Emerson MM. Identification of genes with enriched expression in early developing mouse cone photoreceptors. *Invest Ophthalmol Vis Sci.* 2019;60(8):2787–2799, doi:10.1167/iovs.19-26951.
  68. Dong X, Yang H, Zhou X, et al. LIM-homeodomain transcription factor LHX4 is required for the differentiation of retinal rod bipolar cells and OFF-cone bipolar subtypes. *Cell Rep.* 2020;32(11):108144, doi:10.1016/j.celrep.2020.108144.
  69. Burger CA, Jiang D, Mackin RD, Samuel MA. Development and maintenance of vision's first synapse. *Dev Biol.* 2021;476:218–239, doi:10.1016/j.ydbio.2021.04.001.
  70. Yaron O, Farhy C, Marquardt T, Applebury M, Ashery-Padan R. Notch1 functions to suppress cone-photoreceptor fate specification in the developing mouse retina. *Development.* 2006;133(7):1367–1378, doi:10.1242/dev.02311.
  71. Mizeracka K, DeMaso CR, Cepko CL. Notch1 is required in newly postmitotic cells to inhibit the rod photoreceptor fate. *Development.* 2013;140(15):3188–3197, doi:10.1242/dev.090696.
  72. Chen X, Emerson MM. Notch signaling represses cone photoreceptor formation through the regulation of retinal progenitor cell states. *Sci Rep.* 2021;11(1):14525, doi:10.1038/s41598-021-93692-w.
  73. Nelson BR, Ueki Y, Reardon S, et al. Genome-wide analysis of Müller glial differentiation reveals a requirement for Notch signaling in postmitotic cells to maintain the glial fate. *PLoS One.* 2011;6(8):e22817, doi:10.1371/journal.pone.0022817.
  74. Kelley RA, Chen HY, Swaroop A, Li T. Accelerated development of rod photoreceptors in retinal organoids derived from human pluripotent stem cells by supplementation with 9-cis retinal. *STAR Protoc.* 2020;1(1):100033, doi:10.1016/j.xpro.2020.100033.
  75. Brooks MJ, Chen HY, Kelley RA, et al. Improved retinal organoid differentiation by modulating signaling pathways revealed by comparative transcriptome analyses with development in vivo. *Stem Cell Rep.* 2019;13(5):891–905. Published online October 2019;S2213671119303388, doi:10.1016/j.stemcr.2019.09.009.
  76. Eldred KC, Hadyniak SE, Hussey KA, et al. Thyroid hormone signaling specifies cone subtypes in human retinal organoids. *Science.* 2018;362(6411):eaau6348, doi:10.1126/science.aau6348.
  77. Garita-Hernandez M, Lampič M, Chaffiol A, et al. Restoration of visual function by transplantation of optogenetically engineered photoreceptors. *Nat Commun.* 2019;10(1):4524, doi:10.1038/s41467-019-12330-2.
  78. Gonzalez-Cordero A, Kruczek K, Naeem A, et al. Recapitulation of human retinal development from human pluripotent stem cells generates transplantable populations of cone photoreceptors. *Stem Cell Rep.* 2017;9(3):820–837, doi:10.1016/j.stemcr.2017.07.022.
  79. Dobin A, Davis CA, Schlesinger F, et al. STAR: ultrafast universal RNA-seq aligner. *Bioinformatics.* 2013;29(1):15–21, doi:10.1093/bioinformatics/bts635.
  80. Perampalam P, Dick FA. BEAVR: a browser-based tool for the exploration and visualization of RNA-seq data. *BMC Bioinformatics.* 2020;21(1):221, doi:10.1186/s12859-020-03549-8.
  81. Anders S, Huber W. Differential expression analysis for sequence count data. *Genome Biol.* 2010;11(10):R106, doi:10.1186/gb-2010-11-10-r106.
  82. Blighe K, Rana S, Lewis M. EnhancedVolcano: publication-ready volcano plots with enhanced colouring and labeling. 2021. Available at: <https://github.com/kevinblighe/EnhancedVolcano>. Accessed January 27, 2022.
  83. Yu G, Wang LG, Han Y, He QY. clusterProfiler: an R package for comparing biological themes among gene clusters. *Omics J Integr Biol.* 2012;16(5):284–287, doi:10.1089/omi.2011.0118.